Depolarization of Thomson Scattering Light through Relativistic Effect and Optical Components in ITER

E. Yatsuka[1], T. Hatae[1], K. Ebisawa[2], M. Wakabayashi[2], Y. Kusama[1]

[1] *Japan Atomic Energy Agency, Naka, Ibaraki, Japan*

[2] *K and K Engineering, Kamakura, Kanagawa, Japan*

In ITER, the target of accuracies for electron temperature T_e and electron density n_e profile measurements are 10% and 5%, respectively [1]. In order to collect enough number of photon, some optical components will be installed in the port plug [2]. Since plasmas in ITER emits neutron and gamma-ray, heat is generated in the body of lenses in the port plug due to the nuclear heating. Thus, birefringence of lens arising from the thermal stress occurs, and polarization of the scattered radiation will not be conserved through lenses. On the other hand, spectral density of Thomson scattering is usually considered only the polarized component [3].

For simplicity, we assumed a disk as a lens shape. Heat is removed from the edge of lens by contacting a holder. The difference in refractive indices for radial and azimuthal polarization can be represented as [4]

$$\Delta n = n_r - n_\phi = n_0^3 \frac{\alpha Q}{K} C_B r^2, \tag{1}$$

where n_0, α, Q, K and r denote refractive index at no stress (1.45), thermal coefficient of expansion (5.1×10^{-7} K^{-1}), heat generation rate per unit volume, thermal conductivity (1.5 W/m$\cdot$K) and radius, respectively. The values in brackets represent physical values for fused silica. The coefficient C_B is a function of Poisson's ratio ν and elasto-optical coefficients p_{mn};

$$C_B = \frac{1+\nu}{48(1-\nu)}(p_{11} - p_{12} + 4p_{44}). \tag{2}$$

For fused silica, ν, p_{11}, p_{12} and p_{44} are 0.17, 0.121, 0.270 and -0.075, respectively [5].

To estimate the effect of birefringence roughly, spatial profile of the refractive index variation was ignored, i.e. r was replaced to a typical value of 0.1 m. The difference between radial and azimuthal polarization can be represented as $-1.3 \times 10^{-4} Q$, where Q is in MW/m^{-3}. Figure 1 shows the polarization pupil map for initially horizontal polarized wave, here the thickness of lens d and wavelength λ are assumed to be 50 mm and 633 nm, respectively. From Eq. (1), Figure 1 (a), (b) and (c) correspond to 0.01, 0.03 and 0.05 MW/m^{-3} of heat generation in the lens, respectively. The order of 0.01 MW/m^{-3} of heat generation causes the change of polarization through a lens. The nuclear heating rates in the port plug is evaluated of the order of 0.1 MW/m^{-3} on the mirrors for poloidal polarimeter in ITER [6], which will be installed same port with the edge TS system. Although nuclear heating rate depends on the shielding and so on,

it might not be much less than 0.01 $\mathrm{MW/m^{-3}}$. Thus, the polarization of the scattered radiation might be no longer conserved after the collection optics. We should detect not only polarized component but depolarized ones.

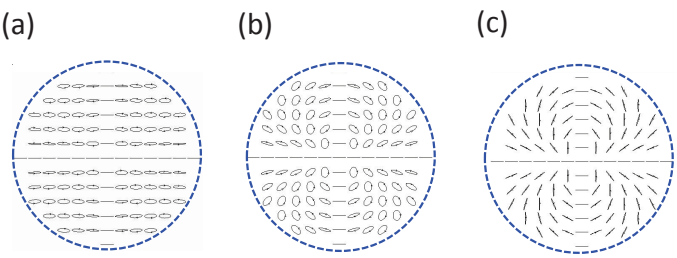

Figure 1: Polarization pupil maps for (a) $\Delta n \cdot d/\lambda = 0.1$, (b) $\Delta n \cdot d/\lambda = 0.3$ and (c) $\Delta n \cdot d/\lambda = 0.5$.

In order to obtain T_e and n_e accurately, the spectral density should be modified to include the contribution of depolarized components. The polarization of scattered radiation from single electron can be evaluated by using a tensor polarizing operator $\overleftrightarrow{\Pi}$:

$$\overleftrightarrow{\Pi} \cdot \hat{\mathbf{e}} = \frac{(1-\beta^2)^{1/2}}{(1-\beta_s)^3} \hat{\mathbf{s}} \times ([\hat{\mathbf{s}} - \hat{\beta}] \times [(1-\beta_i)\hat{\mathbf{e}} - \beta_e \hat{\beta} + \beta_e \hat{\mathbf{i}}]), \tag{3}$$

where $\hat{\mathbf{e}}$, $\hat{\mathbf{s}}$ and $\hat{\mathbf{i}}$ denote the unit vector directing the polarization of incident laser beam, line of sight and propagation of incident laser beam, respectively. And $\hat{\beta}$ denotes electron velocity denominated in the light speed. Let the polarization of the incident laser beam is perpendicular to the scattering plane ($\hat{\mathbf{e}} \cdot \hat{\mathbf{i}} = 0$ and $\hat{\mathbf{e}} \cdot \hat{\mathbf{s}} = 0$), it leads,

$$\begin{aligned} \hat{\mathbf{s}} \times ([\hat{\mathbf{s}} - \hat{\beta}] \times [(1-\beta_i)\hat{\mathbf{e}} - \beta_e \hat{\beta} + \beta_e \hat{\mathbf{i}}]) &= [(1-\cos\theta)\beta_e^2 - (1-\beta_i)(1-\beta_s)]\hat{\mathbf{e}} \\ - \quad \beta_e[\sin\theta + (\beta_k - \beta_s)(1-\cos\theta)]\hat{\mathbf{i}} &+ [\sin\theta\cos\theta - \beta_s \sin\theta - \beta_{k\perp}(1-\cos\theta)](\hat{\mathbf{e}} \times \hat{\mathbf{i}}), \end{aligned} \tag{4}$$

where the second and third terms of right hand side represents the depolarized components. Subscript k and $k\perp$ denote the component parallel and perpendicular (on the scattering plane) to $\mathbf{k}_s - \mathbf{k}_i$, respectively. For convenience, we represent scattered power as a function of normalized wavelength shift $\varepsilon \equiv (\lambda_s - \lambda_i)/\lambda_i$, T_e and θ without integration in the velocity space:

$$\frac{\mathrm{d}^2 P_s}{\mathrm{d}\Omega_s \mathrm{d}\varepsilon} = r_\mathrm{e}^2 \int < S_i > \mathrm{d}^3 r S(\varepsilon, T_\mathrm{e}, \theta), \tag{5}$$

where r_e, $< S_i >$, denote classical electron radius and incident Poynting vector, respectively. We modified the spectral density S to include the contribution from the depolarized components;

$$S(\varepsilon, T_\mathrm{e}, \theta) = S_Z(\varepsilon, T_\mathrm{e}, \theta) \left[q(\varepsilon, T_\mathrm{e}, \theta) + q'(\varepsilon, T_\mathrm{e}, \theta) \right], \tag{6}$$

where S_Z, q and q' denote the spectral density obtained by Zhuravlev [7], density correction factor due to the polarized component [8] and it due to the depolarized components.

Figure 2 (a) shows the ratio of depolarized and polarized contribution as a function of T_e. If electron temperature becomes the order of 10 keV, the order of 1% of correction for the spectral

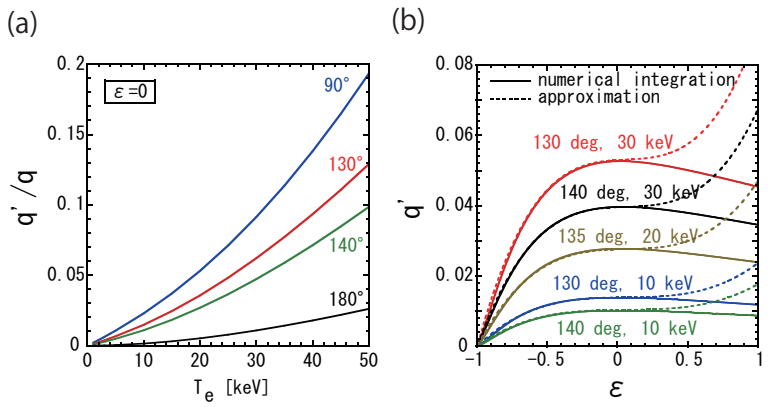

Figure 2: (a) Degree of needed correction of spectral density as a function of T_e and scattering angle θ, (b) Comparison with numerical integration and series expansion forms of q'.

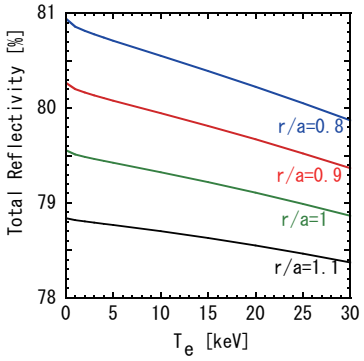

Figure 3: Variation of reflectivity in mirror optics (λ=1064 nm) as a function of T_e.

density is necessary. The effect of depolarized components becomes maximum for approximately 90 degrees of scattering angle, and more than 0.2%/keV of correction is necessary. This value is slightly larger than that obtained by Theimer (1.68% per 10^8 K) [9], which ignores except for the leading term of the depolarized components $\beta_e \sin\theta$. For the practical use in the edge TS system in ITER, we obtained a series expansion form of q' which is valid when T_e<30 keV, 130<θ<140 degrees and -0.6<ε<0 (see Fig. 2 (b)):

$$q' = aT_e(1+bT_e)(1+c\theta)(1+d\varepsilon+e\varepsilon^2+f\varepsilon^3), \tag{7}$$

with $a = 5.16\times10^{-3}$, $b = 1.56\times10^{-2}$, $c = -0.338$, $d = 4.53\times10^{-2}$, $e = -0.153$ and $f = 0.813$, where T_e and θ are in keV and radian, respectively.

Since the reflectivity of a metallic surface depends on the polarization, it indirectly depends on T_e via the depolarization of the scattered radiation. As shown in Fig. 3, variation of reflectivity is approximately up to 0.05%/keV.

The transmissivity of lens also depends on the polarization. Although the dependence on the polarization for a surface is quite small (typically below 0.1%), total transmissivity can be changed of the order of a percent as a function of the polarization. It is

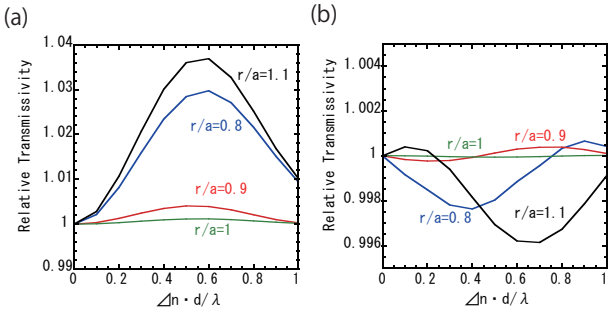

Figure 4: Transmissivity of the lens optics as a function of the induced birefringence for the lens optics: (a) Optical system shown in Ref. [2] and (b) after the reduction of incident angle to lenses.

caused by 34 surfaces from plasma to optical fiber (details of optical system is described in Ref. [2]). Figure 4 (a) shows the transmissivity of the lens optics denominated in it at no stress as a function of the product of induced birefringence and thickness of lens normalized by a wavelength. Here we assumed 633 nm of wavelength, and birefringence occurs at the relay lens in the port plug. In addition, we again ignored the profile of the birefringence for simplicity. The variation of transmissivity depends on the line of sight. On the edge of viewing field of the collection optics, up to 4% of variation may occur. The reason why relative transmissivity is not 1 at $\Delta \cdot d/\lambda = 1$ is due to the curvature of lens and non-zero incident angle to the lens. Actually, the birefringence has a profile, so that it is very hard to predict the transmissivity of lens optics accurately. We modified the optical design of collection optics from Ref. [2] to reduce the incident angle of collected light to lens. First one is replacing the curvature of the relay lens from plano-convex to bi-convex in order to distribute the curvature to 2 surfaces. Second one is reducing the tilting angle of the catadioptric system from the incident light axis. As the result, dependence of polarization on the transmissivity of the lens optics was suppressed up to 0.4% (see Fig. 4 (b)).

In the edge TS system in ITER, the scattered radiation might be depolarized due to the birefringence induced by thermal stress on a lens installed in the port plug. Thus we should include the contribution of depolarized (by relativistic effect in plasma) components to the spectra and reflectivity of mirror optics. They are approximately 0.15%/keV and 0.05%/keV. If T_e becomes of the order of 10 keV, it is not negligible compared with the required accuracy of n_e (5%). Transmissivity of the lens optics will be changed as a function of induced birefringence, which is extremely hard to measure at the plasma discharge. Fortunately, this effect can be suppressed by reducing the incident angle of collected light to lenses.

References

[1] A. J. H. Donné *et al*., Nucl. Fusion **47**, S337 (2007).
[2] E. Yatsuka *et al*., Rev. Sci. Instrm. **81**, 10D541 (2010).
[3] I. H. Hutchinson *Principles of Plasma Diagnostics* Cambridge University Press, Cambridge, (2002)
[4] J. D. Foster and L. M. Osterink, J. Appl. Phys. **41**, 3656 (1970).
[5] R. W. Dixon, J. Appl. Phys. **38**, 5149 (1967).
[6] M. Ishikawa *et al*., Fusion Eng. Des. *In Press* (2011).
[7] V. A. Zhuravlev and G. D. Petrov, Sov. J. Plasma Phys. **5**, 3 (1979).
[8] O. Naito *et al*., Phys. Fluids B **5**, 4256 (1993).
[9] O. Theimer and W. Hicks., Phys. Fluids **11**, 1045 (1968).